

# Shear Behavior of Notched Connection for Glubam-Geopolymer Concrete Composite Structures: Experimental Investigation

Yulin Zhan,<sup>a,b</sup> Wenfeng Huang,<sup>a</sup> Ruizhe Si,<sup>a</sup> Tianyu Xiang,<sup>c,\*</sup> and Liuqing Hao<sup>d</sup>

The glubam (glue-laminated bamboo)-geopolymer concrete composite (BGCC) structure is a possible way to achieve sustainable construction due to its combination of renewable resources and industrial waste. This study combined glubam and geopolymer concrete in composite structures and investigated the shear behavior of BGCC structures with notched connections. Four groups of push-out tests were designed to evaluate the influence of the number of notches and screws on the slip modulus and shear capacity. The results showed that the composite structures with notched connections failed first due to shear cracking at the interface notch. The double-notch specimens increased the shear capacity by 54% compared to single-notch specimens. The shearing bearing capacity rose by 35% on average as a screw increased in a single notch. The ductility and slip modulus were influenced primarily by the screws, with each extra screw in a single notch increasing the slip modulus by 21% in each stage. Based on the test results, a modified formula was proposed to predict the shear-bearing capacity of notched connections in BGCC structures. This study provides comparison data for further studies in the long-term behavior of BGCC structures.

DOI: 10.15376/biores.18.1.701-719

*Keywords:* Glubam; Geopolymer concrete; Composite structures; Notched connection; Shear-bearing capacity; Slip modulus

*Contact information:* a: Dept. of Bridge Engineering, Southwest Jiaotong University, Chengdu 610031 China; b: Institute of Civil Engineering Materials, Southwest Jiaotong University, Chengdu 610031 China; c: Sch. of Architecture and Civil Engineering, Xihua University, Chengdu 610039 China; d: Zigong Academy of Urban Planning & Design Co.Ltd, Zigong 643000 China;

\* Corresponding author: 35132805@qq.com

## INTRODUCTION

Due to the extensive benefits of steel and concrete, steel-concrete composite structures are used widely in building structures. However, issues including the high energy consumption and high pollution in the production process of steel and concrete are becoming unbearable burdens given the current trends toward sustainable development (Hasanbeigi *et al.* 2012). Utilizing recyclable natural resources and industrial wastes as the primary structural materials to replace steel and concrete is a potential way for sustainable development (Shan *et al.* 2017).

It is a demonstrated idea to make full use of renewable resources by using natural renewable wood or bamboo instead of steel in the tensile zone, and inorganic aluminosilicate to prepare inorganic cementitious materials in place of concrete in the compression zone of composite structures (Davidovits 1989; Assi *et al.* 2016).

Glue-laminated bamboo (glubam) is a bamboo-based synthetic material, allowing

large sections and large spans, straight or curved and continuous, providing great plastic property for its application in structural elements (Xiao *et al.* 2010). Glubam has outstanding strength-mass ratio, low dead weight, and great deformation performance. However, the bending stiffness of glubam beam is small due to its low elastic modulus, which greatly limits the span length (Xiao *et al.* 2013). If it can be combined with geopolymer concrete made from industrial waste to form composite beams, the span length can be increased while the environmental impact is reduced.

The geopolymer is produced by a reaction between an aluminosilicate source (precursor) and an alkali solution (*e.g.*, NaOH, KOH) (Khale and Chaudhary 2007). According to Turner and Collins (2013), the carbon emission of 1 m<sup>3</sup> geopolymer concrete in the productive process is only 9% of that of Ordinary Portland Cement (OPC) concrete, which significantly reduces the carbon trace and the impact on the environment. Currently, the major aluminosilicate sources used for the production of the geopolymer are metakaolin (MK), fly ash (FA), ground granulated blast furnace slag (GGBS), and glass powder, *etc.* (Si *et al.* 2020). Among these, fly ash, the primary byproduct of thermal power plants, will pollute the environment if not treated (Singh *et al.* 2022). If utilized as the raw material for the production of geopolymer concrete, it may minimize the production and consumption of OPC while fully using industrial waste, which would help considerably reduce environmental pollution. Furthermore, Olivia and Nikraz (2012) discovered that FA-based geopolymer concrete had stronger flexural and tensile strength than OPC concrete while having a lower elastic modulus. Therefore, FA-based geopolymer can be well applied in the structures as a green binder and an alternative to OPC (Alterary and Marei 2021).

Currently, there are no relevant reports on the composite structures of glubam-geopolymer concrete. However, a significant number of studies on the connection mechanism, flexural performance, long-term performance, and design method of timber-concrete composite (TCC) structures have been conducted by a large number of academics (Clouston *et al.* 2005; Du *et al.* 2019; Jiang *et al.* 2021). These have been widely used in floor structures and bridges (Yeoh *et al.* 2011a), and the shear connectors have been a focus of research, since the service performance of the composite structure depends on the appropriate connection of two materials. The notched connection is one of the common types of shear connection in the TCC system. According to Deam *et al.* (2008), rectangular notched connections with screws can provide great stiffness, strength, and post-peak performance for the structures. In addition to the higher performance of this composite connection, the notched connection reinforced with screws can also effectively improve the bond performance of the interface between concrete and timber due to the shrinkage of concrete (Gutkowski *et al.* 2004). The direction of the timber grain as well as the length and depth of the concrete notch were discovered to be the primary influences on the strength and stiffness of notched connections (Zhang *et al.* 2020).

The bamboo-concrete composite (BCC) beams have also been the subject of some published studies. Different types of shear connections used in BCC structures were investigated *via* push-out tests and bending tests by Shan *et al.* (2017, 2020). The results demonstrated that the notched connection is appropriate for BCC beams due to its high slip modulus and shear strength, while having low ductility. The composite beams with notched connections showed greater secant stiffness and ultimate bearing capacity under short-term loading conditions according to the results of bending tests. Furthermore, the test results for the long-term behavior of BCC beams conducted by Ye *et al.* (2019) showed that the slip modulus and finally slide of notched connections performed better at the service stage when compared to screw connections and steel mesh connections.

As a type of connection appropriate for TCC and BCC structures, concerns have also been raised about the shear carrying capacity, shear stiffness, and other properties of the notched connection, which have been reflected in some standards, *e.g.* NZS 3603 (1993) and Eurocode 5 (2004). It is generally believed that the shear-bearing capacity of the notched connection consists of two parts: the capacity provided by concrete notches and that of the fasteners. Currently, the bearing capacity of each part is determined by the empirical formula based on the experiments, and the applicable conditions are limited. Although the Johnson yield theory has been used to obtain theoretical solutions (Xie *et al.* 2017), its formal complexity limits the application in practice. The notched connection seems to be the most potential type of connection that could be applied to BGCC structures. However, due to the variations in material properties of geopolymers, the structural behavior of BGCC structures with notched connections still needs to be further investigated. In addition, the applicability of the existed prediction methods for the shear-carrying capacity of the notched connection in the BGCC structures also needs to be verified.

This study aimed to investigate the feasibility of utilizing the FA-based geopolymer concrete as a replacement for OPC concrete in the glubam-concrete composite system, and provide comparison data for further studies in the long-term behavior of BGCC structures. Four groups of push-out tests were designed to investigate the structural behavior of the glubam-geopolymer concrete composite system with notched connections. The influence of the number of concrete notches and screws on the failure mode, slip modulus, and shear-bearing capacity of the BGCC system was investigated. According to the test results, the main shear capacity and stiffness of the notched connection were controlled by the concrete plug, which was the same as that in the BCC system (Deam *et al.* 2008; Jiang *et al.* 2020). The screws showed great connection performance in BGCC structures, where it was bent rather than pulled out from the geopolymer concrete slab after loading. A modified formula for calculating the shear capacity of the notched connection of BGCC structures was proposed. Through the validation of pertinent tests, the shear-bearing capacity for notched connection in BCC systems with a satisfactory connection between screws and glubam was predicted using the suggested formula.

## EXPERIMENTAL

### Design of Specimens

Four push-out tests were designed according to the number of screws and notches, named G1-1, G1-2, G2-2, and G2-4, and each group prepared one specimen. The meaning of the specimen number is the number of notches-number of screws, on one side of the push-out specimens, and the G refers to glubam. Table 1 records the number of notches of each specimen, the number of screws inside the notches, and the number of specimens. The push-out test was designed according to the standard push-out test specimen recommended by Eurocode 5 (2004). The geometry and dimensions of the push-out test specimens are depicted in Fig. 1. The geopolymer concrete slabs were positioned on both sides of the glubam element connected with the notched connection. The dimension of the glubam specimens was 250 mm × 250 mm × 400 mm (length × width × height), and the dimension of the geopolymer concrete slabs was 250 mm × 100 mm × 400 mm. The glubam was processed by the factory, and the screw holes with 50 mm in depth were reserved. The notches measured 250 mm × 50 mm × 100 mm. Screws with a diameter of 18 mm and a

length of 180 mm were adopted in this study, 50 mm of which were implanted into the glued bamboo with adhesive, and the remaining 130 mm were anchored in concrete.

**Table 1.** Composition of Connectors

Specimens	Number of Notches	Number of Screws	Number of Specimens
G1-1	1	1	1
G1-2	1	2	1
G2-2	2	2	1
G2-4	2	4	1

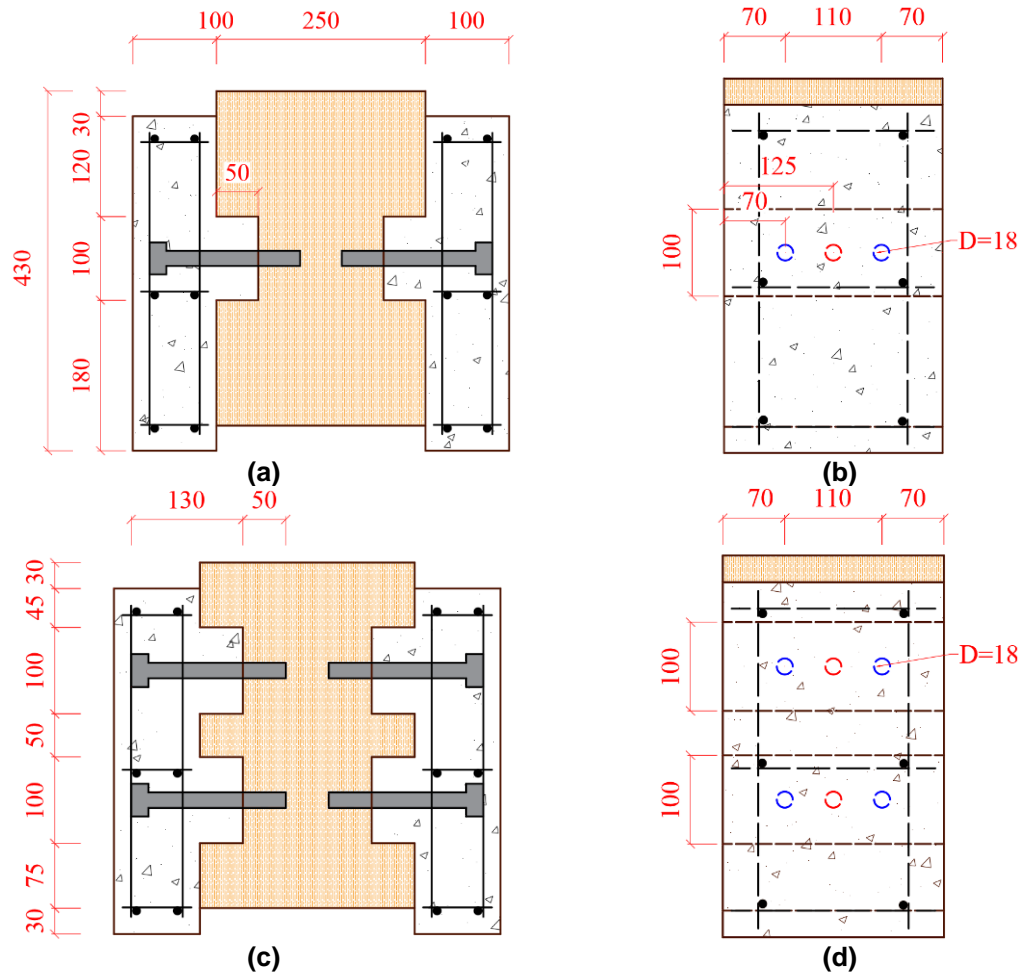


**Fig. 1.** Push-out test specimens (mm): (a) Front view of G1-1 and G1-2; (b) Side view of G1-1 (red) and G1-2 (blue); (c) Front view of G2-2 and G2-4; (d) Side view of G2-2 (red) and G2-4 (blue)

## Materials

### Glubam

Glubam has unique structural characteristics, and the direction of the board's fiber lamination forms three distinct planes (Xiao and Shan 2013). Glubam shows the great bearing capacity and acceptable durability exposure to outdoor conditions with simple protection measures (Shan *et al.* 2011). Fibers of glubam in the longitudinal direction are typically designed four times that for the transverse direction (Shan *et al.* 2017). Consequently, the direction of force is typically not in the transverse direction. The glubam elements were produced in the factory, where the notches of each specimen were processed

according to the design. The mechanical properties of the glubam were tested before the experimental investigation, which is shown in Table 2. The density of the processed glubam is about 0.64 g/cm<sup>3</sup>, and the moisture content is 5.4%. The properties mentioned above were provided by Shanghai Jiyou Building Materials Co., Ltd.

**Table 2.** Mechanical Properties of Glubam (MPa)

Properties	Parallel to Grain				Perpendicular to Grain	
	Tensile	Compressive	Shear	Bending	Tensile	Compressive
Strength	84.53	71.55	13.85	92.56	4.15	16.50
Young's Modulus	7013	9680	8658	7998	-	1867

### *Geopolymer concrete*

The fly ash was adopted as raw material. Na<sub>2</sub>SiO<sub>3</sub> (sodium silicate solution) and NaOH (sodium hydroxide) were used as activators, in which appropriate cement was mixed to prepare fly ash geopolymer concrete. Because the early strength of geopolymer concrete develops slowly at room temperature (Lohani *et al.* 2012), the FA-based geopolymer concrete with 4% Portland cement was used to promote the development of its early strength in this work (Assi *et al.* 2016). Geopolymer concrete has a designed strength of C40, and the mix proportion is indicated in Table 3. During the fabrication of BGCC specimens, 12 cube samples (150 mm × 150 mm × 150 mm) were cast at the same time for the cube compressive strength at different ages, 12 prismatic samples (150 mm × 150 mm × 300 mm) for axial compressive strength and 12 prismatic for elastic modulus, respectively. The mechanical properties (average values) of fly ash geopolymer concrete measured according to GB/T 50081 (2019) are shown in Table 4.

**Table 3.** Mix Proportion of Fly Ash Geopolymer Concrete (kg)

FA	Cement	NaOH Solution	Na <sub>2</sub> SiO <sub>3</sub> Solution	Sand	Gravel
384.0	16.0	45.7	114.3	651.0	1209.0

**Table 4.** Mechanical Properties of FA-based Geopolymer Concrete

Time (day)	Cube Compressive Strength (MPa)	Axial Compressive Strength (MPa)	Elastic Modulus (GPa)
3	24.1	16.7	10.3
7	32.5	23.1	12.7
14	36.5	27.3	15.4
28	42.0	34.7	22.3

### *Screws and rebars*

The 4.8 grade galvanized screws with the nominal yield strength of 320 MPa and ultimate strength of 400 MPa was adopted in this experiment (GB/T 3098.1 2010). The screw was 18 mm in diameter and 180 mm in length, and the hole depth in the glubam was 50 mm. Reinforcements with a diameter of 8 mm were put inside the FA-based geopolymer concrete slab to avoid cracking owing to temperature stress or drying shrinkage during the curing process. The nominal yield strength was 335 MPa, while the elastic modulus of the reinforcements was 210 GPa (GB/T 1499.2 2018).

### *Synthetic glues*

The screws were embedded into the glubam with synthetic glue, *i.e.* a two-component epoxy resin. Agent A is resin, agent B is solidifying agent, and the mass ratio of agent A and agent B is 3:1. The synthetic glue was provided by Shanghai Horse Construction Co., Ltd. Its density after curing is about 1.5 g/cm<sup>3</sup>, and the splitting tensile strength and compressive strength are more than 8.5 and 60 MPa, respectively.

### **Specimen Preparation**

Glubam is a structural composite made of regular bamboo laminas that are glued in overlapping layers parallel to the fibers (Xiao *et al.* 2017). The layers are perpendicular to the concrete slab; that is, the orientation of the reserved screw holes is the transverse direction of the glubam layers. The glubam was uniformly processed at the factory, and the 20 mm-diameter holes with a depth of 50 mm were reserved for screws at the notches. The connection between the screws and the glubam was strengthened by the synthetic glues. Before screwing the screws in, synthetic glues were inserted into the hole to a depth of about 1/3. The specimens were kept indoors for 3 days until the adhesive has fully cured to ensure the effective connection between the screws and the glubam, as shown in Fig. 2. The formwork was set up in accordance with the design dimensions, and the glubam was 30 mm high at the bottom of the formwork to facilitate the test loading. Fly ash-based geopolymer concrete was prepared for this experiment according to the mix proportion. To prevent errors caused by variations in concrete, the same batch of FA-based geopolymer concrete was applied for each test group. The push-out tests were conducted after specimens were cured for 28 days.

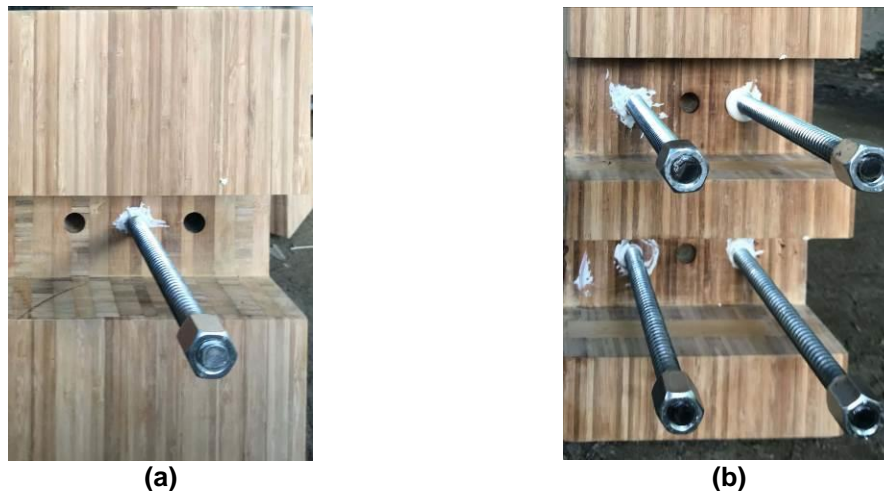


**Fig. 2.** Anchorage of screws: (a) G1-1; (b) G2-4

### **Test Program**

The push-out tests were conducted according to the loading procedure specified in the European standard EN26891 (1991), which were carried out on an electro-hydraulic servo hydraulic press with a minimum stroke of 5 kN/s, as shown in Fig. 3(a). A layer of sand was equally spread on the loading table before the test to flatten the specimen and decrease horizontal friction. The specimens were preloaded to remove the space between the specimens and the loading equipment, which were preloaded to 40% of the estimated failure load and then unloaded to 10% after a pause for 30 s. The load was applied at the

same speed to 70% of the estimated failure load during formal loading and then changed to displacement control until the structure failed. The failure was defined as the residual load dropping to 80% of the peak load or the relative slip exceeding 15 mm, or other phenomena that made continued loading unsafe.

During the test, the load-slip behavior was recorded, as well as the load process and the failure pattern of the BGCC specimens. A load transducer positioned on the top of the specimen measured the load continuously. Four dial indicators with a range of 30 mm were symmetrically set in the middle of the specimen to measure the relative slip, as depicted in Fig. 3(b).



**Fig. 3.** (a) Microcomputer controlled electro-hydraulic servo shear testing machine; (b) Arrangement of dial indicators

## RESULTS AND DISCUSSION

### Loading Process and Failure Mode

The loading procedure of the push-out tests could be separated into 4 stages based on the test phenomena and load-slip curve recorded. The experimental procedure and the phenomenon are shown in Fig. 4, where the red curves in the photographs are the position of the micro-cracks.

When the load was less than 10% of the ultimate in the first stage (part OA), the interface between glubam and geopolymer concrete slab had nearly no relative displacement, and the specimens showed great linear elastic behavior. In the second stage (part AB), the relative slip progressively increased with applying of the load, and micro-cracks formed at the interface between the glubam and geopolymer concrete slabs. When the load was 50% of the ultimate (point B), micro-cracks appeared at the notches. In the third stage (part BC), when the load continued to increase to 90% of the ultimate, micro-cracks between the glubam and geopolymer concrete slabs developed and finally penetrated. The microcracks in concrete at the notches grew from top to bottom, and the specimens reached the plastic stage. In the fourth stage (part CD), the concrete micro-cracks in the notches converged to create continuous cracks when close to the ultimate load, generating a slight angle with the interface, and the width of cracks steadily grew and exceeded 2 mm until failure.



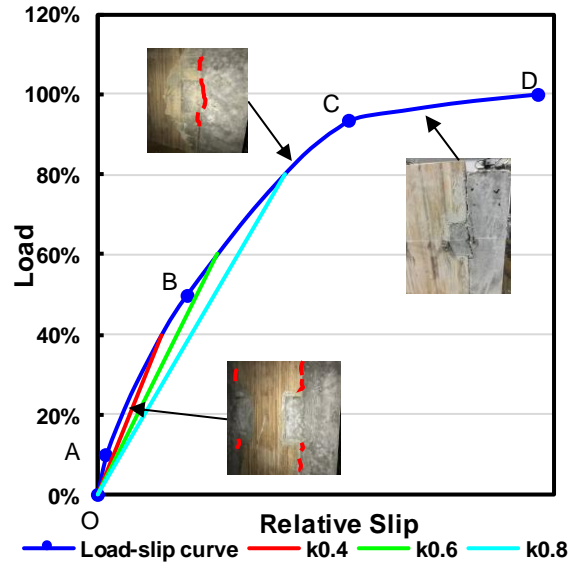


Fig. 4. Typical loading process

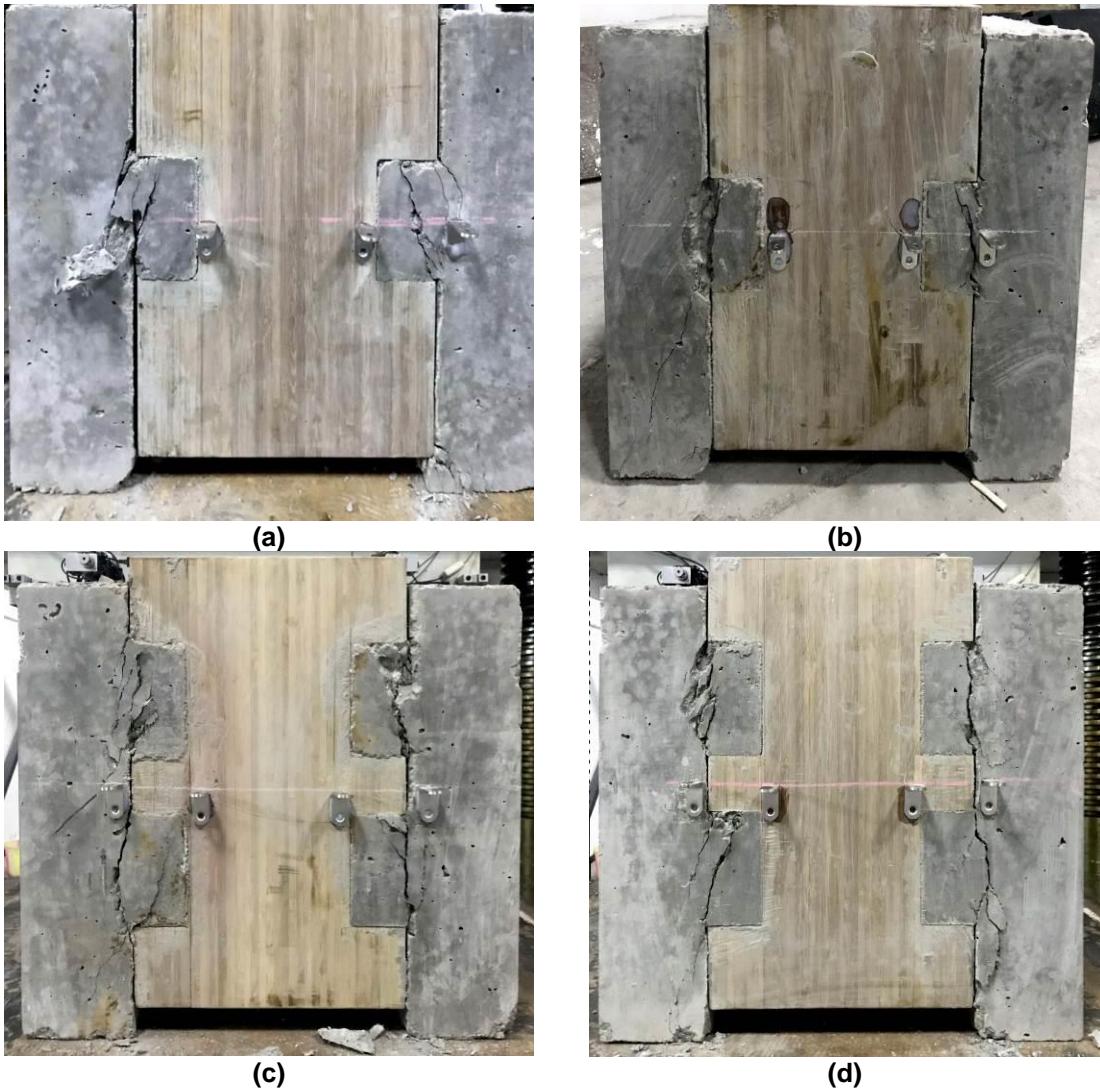


Fig. 5. Failure modes of specimens: (a) G1-1; (b) G1-2; (c) G2-2; (d) G2-4





**Fig. 6.** Intact connection between screws and glubam

The failure of BGCC structures with a notched connection was caused by the shear failure of the geopolymer concrete near the notches. Typical failure modes of each group of specimens are shown in Fig. 5. No evident damage was observed in the glubam after the complete collapse of the specimens. The concrete was cut after loading to evaluate the connection between the screws and the glubam, as shown in Fig. 6. The screws had been bent upward rather than pulled out from the geopolymer concrete slab after loading while the connection with glubam was still solid. This kind of failure mode was also observed in the experimental research of Jiang *et al.* (2020) and Xie *et al.* (2017).

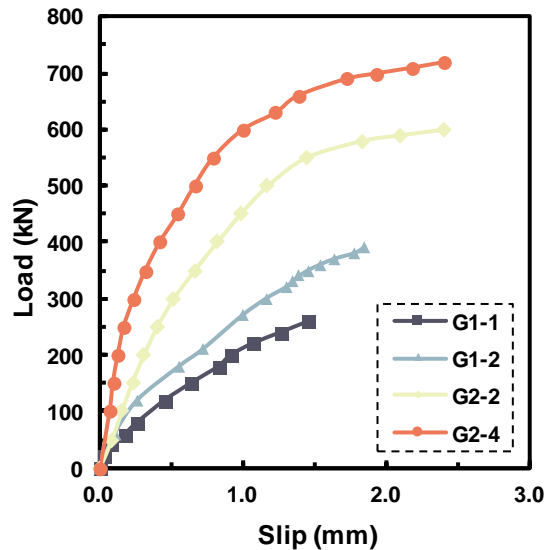
### Load-slip Relations

The load-slip curves of the four specimens are shown in Fig. 7. Throughout the loading process, all specimens demonstrated a consistent load-slip relationship. The interface slip grew linearly with the load in the beginning of loading. The slope of each curve decreased as the load grew until the failure of specimens. Double-notch specimens exhibited more obvious nonlinear behavior than single-notch specimens in the late stage of loading, especially after reaching about 80% of the ultimate load. However, no evident decline was found in any of the specimen curves. Overall, the load-slip curve of the single-notch groups basically changed linearly, and the specimens tended to brittle failure. The load-slip curve of the double-notch groups revealed a rather clear plasticity, with ductile failure characteristics.

Table 5 shows the ultimate bearing capacity of each specimen as well as the secant modulus corresponding to 40%, 60%, and 80% ultimate load, respectively. The ultimate carrying capacity was provided by the notched connection on both sides. The secant modulus  $K$  was determined by the ratio of the load to the corresponding slip, which was a reliable parameter to evaluate the slip modulus of BGCC specimens (Shan *et al.* 2017). The secant modulus of  $k_{0.4}$ ,  $k_{0.6}$ , and  $k_{0.8}$  are referred to the service, ultimate, and near-collapse load levels, respectively (Shan *et al.* 2017), which were obtained using the secant lines as shown in Fig. 4.

**Table 5.** Push-out Test Results of BGCC Structures

Specimens	Shear Strength (kN)	Ultimate Slip (mm)	$k_{0.4}$	$k_{0.6}$	$k_{0.8}$
			(kN/mm)	(kN/mm)	(kN/mm)
G1-1	260	1.46	233.3	212.4	203.3
G1-2	390	1.84	288.9	255.1	241.0
G2-2	600	2.39	451.8	380.6	352.9
G2-4	720	2.4	761.3	530.4	460.6

**Fig. 7.** Load-slip curves

### Shear Bearing Capacity

Shear connection with sufficient strength is the crucial assurance for the efficient connection of steel and concrete. It is critical to determine the impact of various parameters on the ultimate bearing capacity. The influence of the number of notches on the ultimate bearing capacity was first compared and examined. By comparing the test results of single-notch series G1-2 and double-notch series G2-2 without changing the number of screws, the effect of the number of notches on the notched connection could be evaluated. The experimental results revealed that increasing the number of notches enhanced the shear capacity of the specimens with two screws by 54%, due to the larger shear area of concrete notches compared to the single-notch, which is consistent with the research results of Yeoh *et al.* (2011b). In this test, the shear area provided by the double-notch specimen was about  $5 \times 10^4 \text{ mm}^2$ , which was twice that of the single ones. However, the bearing capacity did not increase as much as the shear area. The most likely reasons are the quantity and layout of screws in each notch, which will be discussed further later. In general, the shear-bearing capacity would be effectively improved with the increase of the number of notches. This result is consistent with BCC structures using normal concrete (Deam *et al.* 2008; Jiang *et al.* 2020).

The ultimate loads of G1-1 and G2-2, G1-2, and G2-4 groups were compared, since the number of screws in a single notch could affect shear capacity. When the notch and screw were both increased, the specimen's shear capacity was almost doubled. G1-1 and G1-2 groups with the same number of notches but the different number of screws, as well as G2-2 and G2-4 groups, were compared to clarify the impact of the number of screws on

shear-carrying capacity, as illustrated in Fig. 8. In conclusion, increasing the number of screws improved the bearing capacity of the notched connection. The shear-bearing capacity of G1-1 and G1-2 with single notch rose by 130 kN, an increase of 50%, as the number of screws increased. For G2-2 and G2-4 groups with double notches, the shear capacity of the connectors was enhanced by 20% (120 kN). It was demonstrated that the proportion of shear capacity provided by the screws was reduced as the number of notches increased. According to concrete shear failure modes, the shear area of the notches was still the most important factor affecting shear capacity in the glubam-geopolymer concrete composite structures. The presence of screws was more important to prevent the sudden collapse of concrete and improve the specimen's ductility (Deam *et al.* 2008). Nevertheless, the shear-carrying capacity provided by screws could not be ignored.

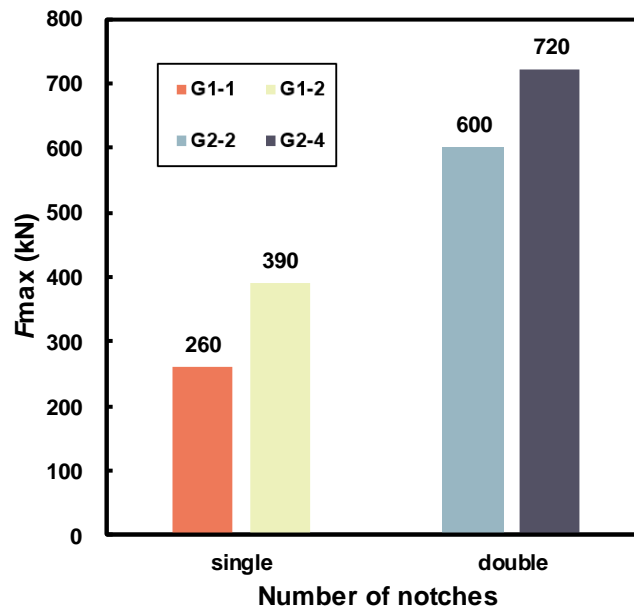


Fig. 8. Effect of screw number on shear-bearing capacity

### Slip Modulus

To limit the deformation of the structures during normal conditions, the notched connection should have a sufficient slip modulus. In this paper,  $k_{0.4}$ ,  $k_{0.6}$ , and  $k_{0.8}$  are used to evaluate the effect of the number of notches and screws on the slip modulus (EN 26891 1991). Figure 9 depicts the calculated results. According to the test results of G1-2 and G2-2 groups, the slip modulus at each stage was increased by 51% on average with the number of notches growing. For groups G1-1 and G1-2, G2-2, and G2-4 with the same number of notches, the slip modulus at each stage was significantly improved with the increase of the number of screws in the notches. Both single and double-notch specimens essentially showed the same rule, where the slip modulus was increased by 21% when an additional screw was added in a single notch. Similarly, the test results of the G1-2 and G2-4 groups, as well as the G1-1 and G2-2 groups, were compared in order to rule out the impact of variations in the number of screws in a single notch. The results demonstrated that increasing the screw and notch at the same time increased the slip modulus of the G1-1 and G1-2 specimens by 82 and 121% at each stage on average, respectively. The screws improve the slip modulus at each stage, the postpeak behavior, and the ductile behavior (Yeoh *et al.* 2011b).

In combination with the load-slip curves depicted in Fig. 7, the slip modulus dropped as the load increased, and the greater the decrease of  $k_{0.8}$  compared with the initial slip modulus, the better ductility of the notched connection. The ductility behavior could be enhanced by increasing the number of notches and screws, as evidenced by the change of slip modulus of each specimen in Fig. 10. The vertical coordinate is the ratio of the slip modulus of each stage to the normal service stage.

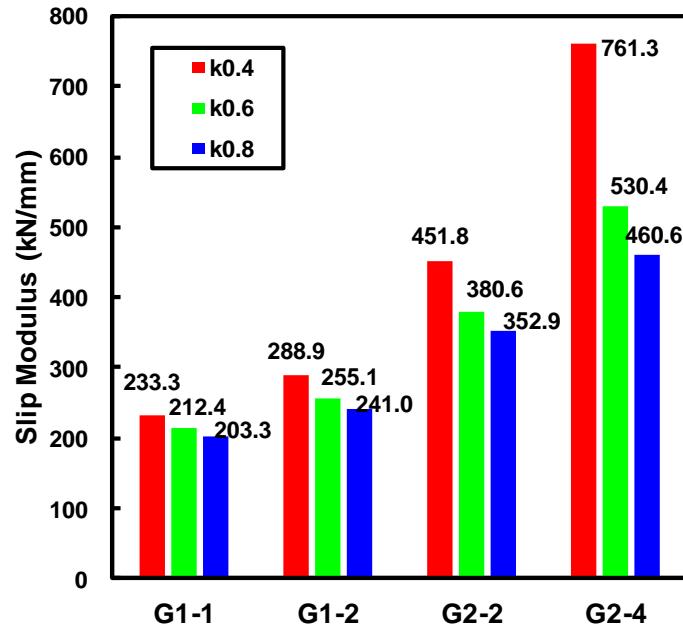


Fig. 9. Slip modulus of all specimens

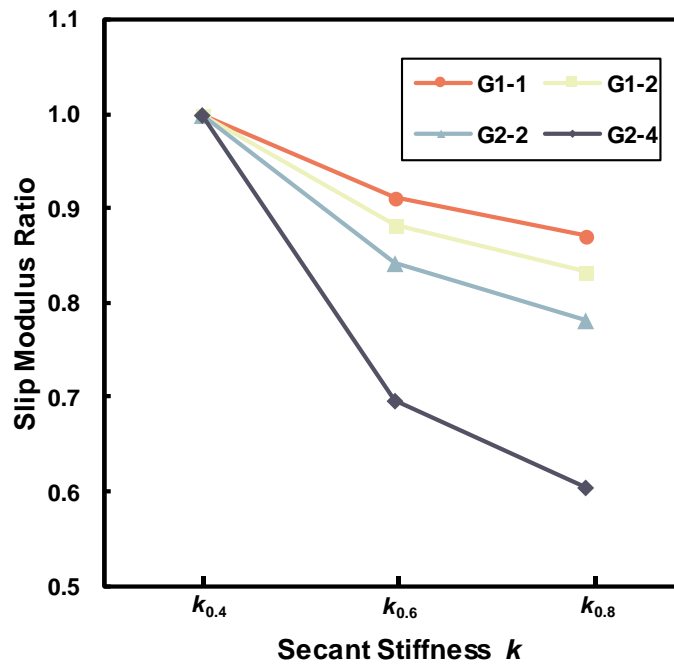


Fig. 10. Reduction of slip modulus

## PREDICTION OF THE SHEAR-BEARING CAPACITY

### Calculating Method

There have been a number of studies on the various connection used in BCC structures; however, a unified formula for estimating the slip modulus and capacity of notched connections has not been established (Jiang *et al.* 2017; Xie *et al.* 2017). In this work, a method for calculating the shear capacity of notched connection of glulam geopolymer concrete composite structures is proposed by referring to a large number of studies in the TCC and BCC structures, as well as the recommendations given by Eurocodes. To verify the formula proposed in this work, the relevant research results were selected and compared with the calculated values.

Methods for predicting the shear capacity of notched connection were considered and compared with the results of this test, including the *EC\* method* proposed by Yeoh *et al.* (2011b) considering the reduction factor  $\beta^*$ , the *NZS method* adopted by New Zealand Standards for both timber (NZS 3603 1993) and concrete structures (NZS 3101 2006), and the *Xie's method* deduced by Xie *et al.* (2017) based on Johansen yield theory.

The *EC\* method* is proposed by Yeoh *et al.* (2011b) to calculate the shear capacity of notched connection with modified shear reduction factor  $\beta^*$  based on the Eurocodes for both timber (EN 1995-1-1 2004) and concrete structures (EN 1992-1-1 2004). According to Yeoh *et al.* (2011b), the notch length  $l_n$  had a great impact on the ultimate bearing capacity of the connection. In order to account for the influence of loading distance, notch length, and the diameter of the lag screw, a new reduction factor  $\beta^*$  is proposed to replace  $\beta$  in the original formula. The shear strength of concrete for a notched connection reinforced with a screw can be calculated with Eq. 1.

$$F_1 = \beta^* 0.5 b_n l_n v f_c + n_{ef} (l_{ef} d_{ef} \pi)^{0.8} f_w \quad (1)$$

where  $\beta^*$  is the modified shear reduction factor, which can be calculated according to Eq. 2;  $b_n$  and  $l_n$  represent the width and length of the notch, respectively. The parameter  $v$  represents the strength reduction factor of concrete cracking under shear;  $f_c$  corresponds to the compressive strength of concrete;  $n_{ef}$  corresponds to the effective number of screws;  $d$  denotes the diameter of the screw;  $l_{ef}$  denotes screw embedment depth minus screw diameter; and  $f_w$  indicates the pulling strength of the screw.

$$\beta^* = \frac{l_n - 2d}{2l_n} \quad (2)$$

The *NZS method* is a New Zealand standard for calculating the shear capacity of notched connections (NZS 3603 1993). According to the shear failure mode of concrete notches and pulling out of screws, the following equation is used to calculate the shear capacity of notched connection,

$$F_2 = 0.2 f_c b_n l_n + n_{ef} k_1 p f_w \quad (3)$$

where  $k_1$  is the correction coefficient of load on timber beam;  $p$  denotes screw embedding depth.

Xie *et al.* (2017) established the shear capacity calculation formula of the notched connection of the TCC structures based on the Johansen yield theory, as follows,

$$F_3 = \gamma f_w d (l - p - b_2) + 0.51 \sqrt{f_c} b_n l_n \quad (4)$$

where  $\gamma$  is the ratio of the embedded strength of the screws in concrete to that of in timber. The parameters  $f_w$  and  $f_{hc}$  are embedded strengths of the screws in timber and concrete, which can be calculated according to Eqs. 5 and 6, respectively.  $E_{cm}$  corresponds to the elastic modulus of concrete;  $\rho_k$  represents the density of the timber; and  $l$  refers to the total length of the screw. It is worth noting that this model is tailored to take characteristic values of shear-bearing capacity.

$$f_{h,c} = \frac{0.29d^2 \sqrt{f_c E_{cm}}}{dh} \quad (5)$$

$$f_{h,t} = 0.082(1 - 0.01d) \rho_k \quad (6)$$

### Modification of Prediction Formula

The notches and the screws make up the shear-bearing capacity of the notched connection. In a number of suggested formulas mentioned in Section 4.1, the shear capacity provided by the screw is related to its tensile capacity. However, according to the failure mode of the notched connection in this test, it was suggested that screws bent after the shear failure of concrete plugs. Pull-out failure may happen if the length of the screw embedment is not enough. However, in terms of the shear capacity of screws with a reliable connection to glulam and concrete, it is recommended to adopt the formula for calculating the shear capacity of screws suggested in Eurocode 4 (2005). Since the screws were not completely sheared when the specimens collapsed, the ultimate strength of the screws in the formula was replaced by the yield strength, as shown in Eq. 7. The calculation method suggested by Yeoh *et al.* (2011b) for the contribution of geopolymer concrete plugs to shear-bearing capacity is still adopted, because this model took into account the reduction in concrete strength caused by shear cracking. Finally, it is recommended to determine the shear-bearing capacity of the notched connection according to Eq. 8, where  $f_y$  is the yield strength of the screws and  $\gamma_v$  is the partial factor. The results of calculation and comparison are shown in Table 6, which are drawn in Fig. 10 for ease of comparison.

$$N_v = 0.8A_s f_y / \gamma_v \quad (7)$$

$$F_4 = \beta^* 0.5b_n l_n v f_c + 0.8A_s f_y / \gamma_v \quad (8)$$

**Table 6.** The Shear Capacity Calculated with Each Formula

Specimens	$F_1(\text{test})$	EC* method		Xie's method		NZS method		Modified formula		
		$F_1$	$F_1/F_1$	$F_2$	$F_2/F_1$	$F_3$	$F_3/F_1$	$F_4$	$F_4/F_1$	SD
G1-1	260.0	325.0	1.25	320.3	1.23	375.8	1.45	256.9	0.99	0.07
G1-2	390.0	497.2	1.27	397.9	1.02	381.7	0.98	361.1	0.93	
G2-2	600.0	650.0	1.08	640.6	1.07	745.8	1.24	513.8	0.86	
G2-4	720.0	994.5	1.38	795.7	1.11	751.7	1.04	722.2	1.00	



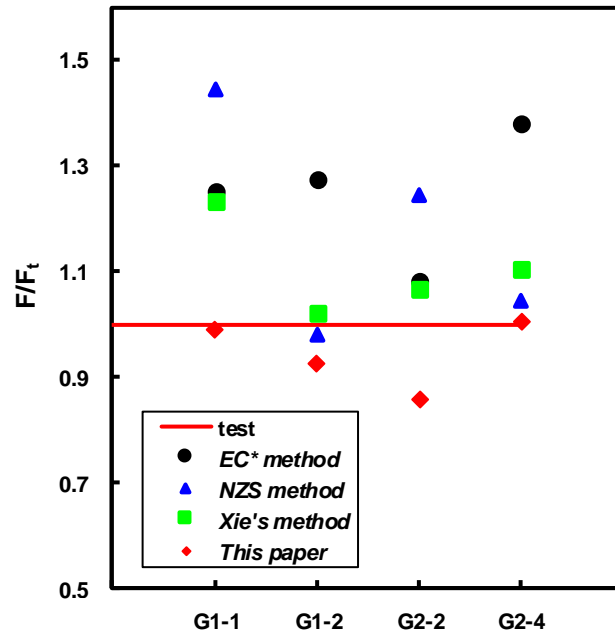


Fig. 11. Comparison between calculation and test results

**Validation**

To validate the modified formula suggested in this paper, a number of references were found in which the screws were well fastened to glulam or timber and eventually bent in the test (Xie *et al.* 2017; Jiang *et al.* 2020). It is worth noting that the yield strength of screws was adopted to determine the shear capacity, and the conclusion was biased toward safety. In addition, the structure size and material strength utilized for the calculation were all from the references. The data is shown in Table 7, where  $D$  is the diameter of screws,  $F$  refers to the calculated value according to Eq. 8, and  $F'_t$  corresponds to the test results in the references (shear capacity provided by the single-side notched connection). The mean value of  $F/F'_t$  was 0.88, and the standard deviation was 0.07, indicating that the prediction formula provided a stable and reliable prediction of shear-carrying capacity.

**Table 7.** Validation of Recommended Formula

Ref.	Specimens	Height (mm)	Width (mm)	Depth (mm)	$D$ (mm)	$F$ (kN)	$F'_t$ (kN)	$F/F'_t$	Average	SD
Xie <i>et al.</i> (2017)	T-1	150	60	50	16	69.6	90.2	0.77	0.88	0.07
	T-2	150	60	20	16	69.6	77.7	0.90		
	T-3	150	40	50	16	60.1	64.1	0.94		
	T-4	150	80	50	16	79.0	93.7	0.84		
	T-5	150	60	50	13	57.0	61.2	0.93		
	T-6	150	60	50	10	47.4	56.9	0.83		
Jiang <i>et al.</i> (2020)	LC-NS-3	150	150	50	16	111.8	117.6	0.95		

## CONCLUSIONS

1. The failure of glubam-geopolymer concrete composite (BGCC) structures with notched connections started from the shear cracking of geopolymer concrete at the notches. The specimens with single-notch failed suddenly showing a brittle failure characteristic, while the specimen with double-notch exhibited good ductility. The screws bent upward along the anchorage after the specimen failed, yet the glubam showed no evident damage.
2. The notched connection is suitable for BGCC structures. However, sufficient screws are needed in the notches to ensure the bearing capacity of the connection. The shearing bearing capacity rose by 50% as screws increased in single-notch specimens. For specimens with double-notch, the shear capacity was increased by 20%, which demonstrated the reducing contribution of screws as the number of notches increased.
3. The slip modulus of the notched connection was increased with an increase in the number of screws. In each stage, adding a screw in a single-notch raised the slip modulus by 21%. Nevertheless, the ductility behavior could be enhanced by increasing both the number of notches and screws. Although the notches showed a greater improvement on the slip modulus than screws, the number of notches should not be increased blindly due to the limited glubam-concrete contact interface.
4. Based on the analysis of test results and the combination of the related calculating methods, a modified prediction formula for the shear-bearing capacity of the notched connection with an adequate connection between the screws and the glubam was proposed in this paper, which was suitable for the condition that the screws were well connected with the glubam and the screws were not pulled out. The ratio of the predicted capacity to relate test results was 0.88 on average, and the standard deviation was 0.07, indicating that the modified method provides a stable and reliable prediction of shear-bearing capacity.

## ACKNOWLEDGEMENTS

The research described in this paper was supported by The National Natural Science Foundation of China (Grants 51878564 and 52278220) and Sichuan Science and Technology Program (Grant 2021JDTD0012), and the National Key Research and Development Program of China (Grant 2016YFB1200401) is gratefully acknowledged.

## REFERENCES CITED

- Alterary, S. S., and Marei, N. H. (2021). "Fly ash properties, characterization, and applications: A review," *Journal of King Saud University Science* 33(6). DOI: 10.1016/j.jksus.2021.101536
- Assi, L., Ghahari, S., Deaver, E. E., Leaphart, D., and Ziehl, P. (2016). "Improvement of the early and final compressive strength of fly ash-based geopolymer concrete at ambient conditions," *Construction and Building Materials* 123, 806-813. DOI: 10.1016/j.conbuildmat.2016.07.069

- Clouston, P., Bathon, L. A., and Schreyer, A. (2005). "Shear and bending performance of a novel wood-concrete composite system," *Journal of Structural Engineering* 131(9), 1404-1412. DOI: 10.1061/(asce)0733-9445(2005)131:9(1404)
- Davidovits, J. (1989). "Geopolymers and geopolymeric materials," *Journal of Thermal Analysis* 35(2), 429-441.
- Deam, B. L., Fragiaco, M., and Buchanan, A. H. (2008). "Connections for composite concrete slab and LVL flooring systems," *Materials and Structures* 41(3), 495-507. DOI: 10.1617/s11527-007-9261-x
- Du, H., Hu, X. M., Jiang, Y. C., Wei, C. Y., and Hong, W. (2019). "Load-carrying capacity of self-tapping lag screws for glulam-lightweight concrete composite beams," *BioResources* 14(1), 166-179. DOI: 10.15376/biores.14.1.166-179
- EN 1992-1-1: Eurocode 2 (2004). "Design of concrete structures – Part 1-1: General rules and rules for buildings," European committee for standardization, Brussels, Belgium.
- EN 1994-2: Eurocode 4 (2005). "Design of composite steel and concrete structures – Part 2: General rules and rules for bridges," European Committee for Standardization, Brussels, Belgium.
- EN 1995-1-1: Eurocode 5 (2004). "Design of timber structures – Part 1-1: Common rules and rules for buildings," European Committee for Standardization, Brussels, Belgium.
- EN 26891 (1991). "Timber structures joints made with mechanical fasteners – General principles for the determination of strength and deformation characteristics," European Committee for Standardization, Brussels, Belgium.
- GB/T 1499.2 (2018). "Chinese standard: Steel for the reinforcement of concrete – Part 2: Hot rolled ribbed bars," General Administration of Quality Supervision, Inspection and Quarantine PRC, Beijing, China.
- GB/T 3098.1 (2010). "Chinese standard: Mechanical properties of fasteners – Bolts, screws and studs," Standardization Administration of China, Beijing, China.
- GB/T 50081 (2019). "Chinese Standard: Standard for test methods of concrete physical and mechanical properties," Ministry of Housing and Urban-Rural Development PRC, Beijing, China.
- Gutkowski, R. M., Brown, K., Shigidi, A., and Natterer, J. (2004). "Investigation of notched composite wood-concrete connections," *Journal of Structural Engineering* 130(10), 1553-1561. DOI: 10.1061/(asce)0733-9445(2004)130:10(1553)
- Hasanbeigi, A., Price, L., and Lin, E. (2012). "Emerging energy-efficiency and CO<sub>2</sub> emission-reduction technologies for cement and concrete production: A technical review," *Renewable & Sustainable Energy Reviews* 16(8), 6220-6238. DOI: 10.1016/j.rser.2012.07.019
- Jiang, Y. C., Hong, W., Hu, X. M., Crocetti, R., Wang, L., and Sun, W. M. (2017). "Early-age performance of lag screw shear connections for glulam-lightweight concrete composite beams," *Construction and Building Materials* 151 36-42. DOI: 10.1016/j.conbuildmat.2017.06.063
- Jiang, Y. C., Hu, X. M., Hong, W., Zhang, J., and He, F. Q. (2020). "Experimental study on notched connectors for glulam-lightweight concrete composite beams," *BioResources* 15(2), 2171-2180. DOI: 10.15376/biores.15.2.2171-2180
- Jiang, Y. C., Hu, X. M., Liu, Y., and Tao, L. (2021). "Long-term performance of glulam-lightweight concrete composite beams with screw connections," *Construction and Building Materials* 310. DOI: 10.1016/j.conbuildmat.2021.125227
- Khale, D., and Chaudhary, R. (2007). "Mechanism of geopolymerization and factors

- influencing its development: A review,” *Journal of Materials Science* 42(3), 729-746. DOI: 10.1007/s10853-006-0401-4
- Lohani, T., Jena, S., Dash, K., and Padhy, M. (2012). “An experimental approach on geopolymeric recycled concrete using partial replacement of industrial byproduct,” *International Journal of Civil & Structural Engineering* 3(1), 141-149.
- NZS 3101 (2006). “New Zealand Standard: Concrete structures standard, Part 1: The design of concrete structures,” SNZ Standards New Zealand.
- NZS 3603 (1993). “New Zealand Standard: Design timber structures,” SNZ Standards New Zealand.
- Olivia, M., and Nikraz, H. (2012). “Properties of fly ash geopolymer concrete designed by Taguchi method,” *Materials & Design* 36 191-198. DOI: 10.1016/j.matdes.2011.10.036
- Shan, B., Chen, J., and Xiao, Y. (2011). “Mechanical properties of glubam sheets after artificial accelerated aging,” *13<sup>th</sup> International Conference on Non-Conventional Materials and Technologies*, Changsha, China.
- Shan, B., Xiao, Y., Zhang, W.L., and Liu, B. (2017). “Mechanical behavior of connections for glubam-concrete composite beams,” *Construction and Building Materials* 143 158-168. DOI: 10.1016/j.conbuildmat.2017.03.136
- Shan, B., Wang, Z., Li, T., and Xiao, Y. (2020). “Experimental and analytical investigations on short-term behavior of glubam-concrete composite beams,” *Journal of Structural Engineering* 146(3), article 04019217. DOI: 10.1061/(ASCE)ST.1943-541X.0002517
- Si, R. Z., Guo, S. C., Dai, Q. L., and Wang, J. Q. (2020). “Atomic-structure, microstructure and mechanical properties of glass powder modified metakaolin-based geopolymer,” *Construction and Building Materials* 254. DOI: 10.1016/j.conbuildmat.2020.119303
- Singh, N. B., Agarwal, A., De, A., and Singh, P. (2022). “Coal fly ash: An emerging material for water remediation,” *International Journal of Coal Science & Technology* 9(1). DOI: 10.1007/s40789-022-00512-1
- Turner, L. K., and Collins, F. G. (2013). “Carbon dioxide equivalent (CO<sub>2</sub>-e) emissions: A comparison between geopolymer and OPC cement concrete,” *Construction and Building Materials* 43 125-130. DOI: 10.1016/j.conbuildmat.2013.01.023
- Xiao, Y., and Shan, B. (2013). *Modern Bamboo Structures*, China Architecture and Building Press, Beijing.
- Xiao, Y., Yang, R. Z., and Shan, B. (2013). “Production, environmental impact and mechanical properties of glubam,” *Construction and Building Materials* 44 765-773. DOI: 10.1016/j.conbuildmat.2013.03.087
- Xiao, Y., Zhou, Q., and Shan, B. (2010). “Design and construction of modern bamboo bridges,” *Journal of Bridge Engineering* 15(5), 533-541. DOI: 10.1061/(asce)be.1943-5592.0000089
- Xiao, Y., Wu, Y., Li, J., and Yang, R. Z. (2017). “An experimental study on shear strength of glubam,” *Construction and Building Materials* 150 490-500. DOI: 10.1016/j.conbuildmat.2017.06.005
- Xie, L., He, G. J., Wang, X. D., Gustafsson, P. J., Crocetti, R., Chen, L. P., Li, L., and Xie, W. H. (2017). “Shear capacity of stud-groove connector in glulam-concrete composite structure,” *BioResources* 12(3), 4690-4706. DOI: 10.15376/biores.12.3.4960-4706
- Ye, X., Shan, B., Yue, Q., and Wang, Z. Y. (2019). “Long-term behavior of connections

- for glulam-concrete composite beams,” *1<sup>st</sup> International Conference on Advances in Civil Engineering and Materials (ACEM) / 1<sup>st</sup> World Symposium on Sustainable Bio-Composite Materials and Structures (SBMS)*, Nanjing Forestry Univ, Nanjing, Peoples R China, 2019 Nov 09-11. DOI: 10.1051/mateconf/201927501001
- Yeoh, D., Fragiacomio, M., De Franceschi, M., and Boon, K. H. (2011a). “State of the art on timber-concrete composite structures: Literature review,” *Journal of Structural Engineering*. 137(10), 1085-1095. DOI: 10.1061/(asce)st.1943-541x.0000353
- Yeoh, D., Fragiacomio, M., De Franceschi, M., and Buchanan, A. H. (2011b). “Experimental tests of notched and plate connectors for LVL-concrete composite beams,” *Journal of Structural Engineering* 137(2), 261-269. DOI: 10.1061/(asce)st.1943-541x.0000288
- Zhang, L., Chui, Y. H., and Tomlinson, D. (2020). “Experimental investigation on the shear properties of notched connections in mass timber panel-concrete composite floors,” *Construction and Building Materials* 234, article 117375. DOI: 10.1016/j.conbuildmat.2019.117375

Article submitted: October 12, 2022; Peer review completed: November 5, 2022; Revised version received: November 14, 2022; Accepted: November 15, 2022; Published: November 23, 2022.

DOI: 10.15376/biores.18.1.701-719